Supplemental Materials

Molecular Biology of the Cell

Bartolini et al.

Supplemental Figure Legends

Figure S1

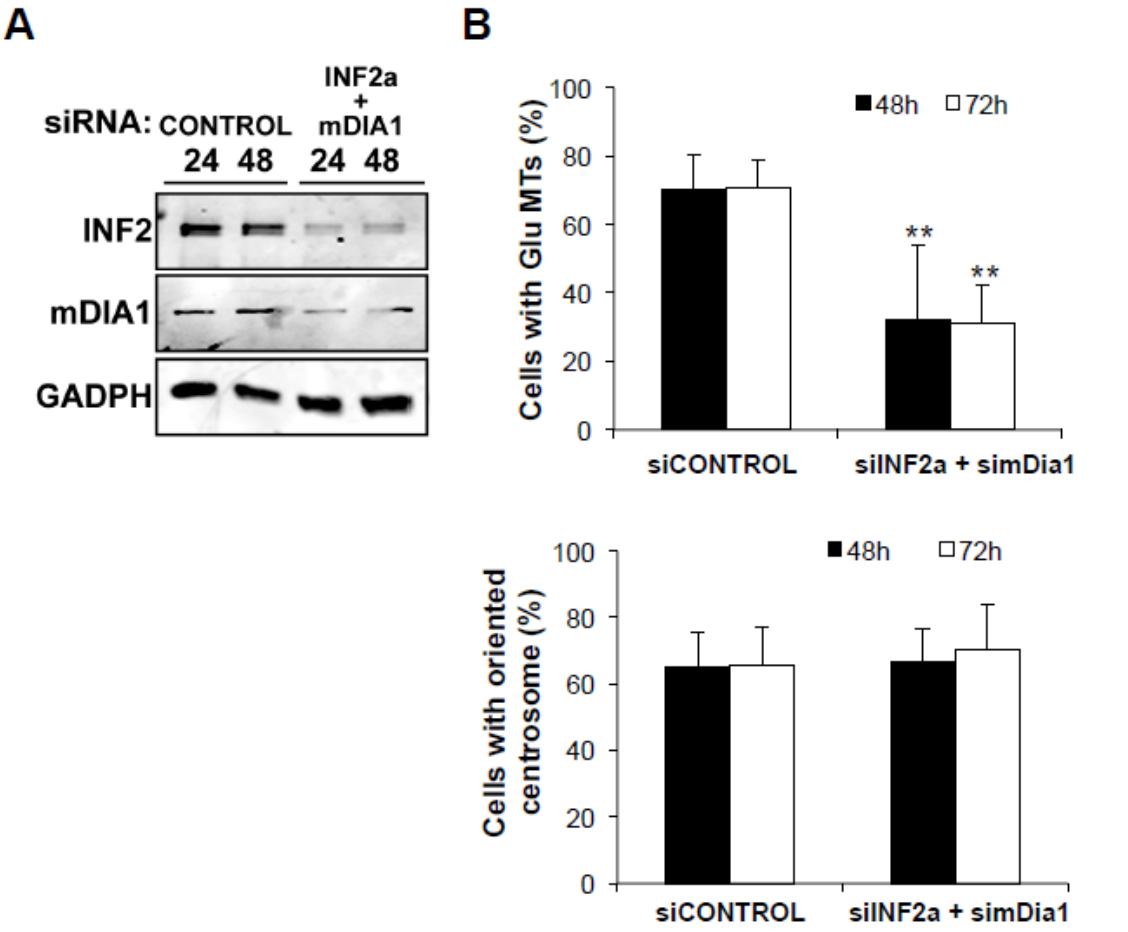

Figure S1. Effects of combined mDia1 and INF2 knockdown on Glu MT levels and centrosome orientationin NIH3T3 fibroblasts. (A) Immunoblot analysis of INF2, mDia1 and GAPDH (loading control) in NIH3T3 fibroblasts treated with control or mDia1 and INF2 siRNAs for the indicated times (h). (B) Quantification of cells with Glu MTs (upper histogram) or oriented centrosome (lower histogram) that had been treated as in (A). Control is non-coding siRNA. Data are mean $\pm$ SD from four independent experiments (n> 200 cells/experiment).**, $p<0.001$ calculated by chi-square test.

Figure S2

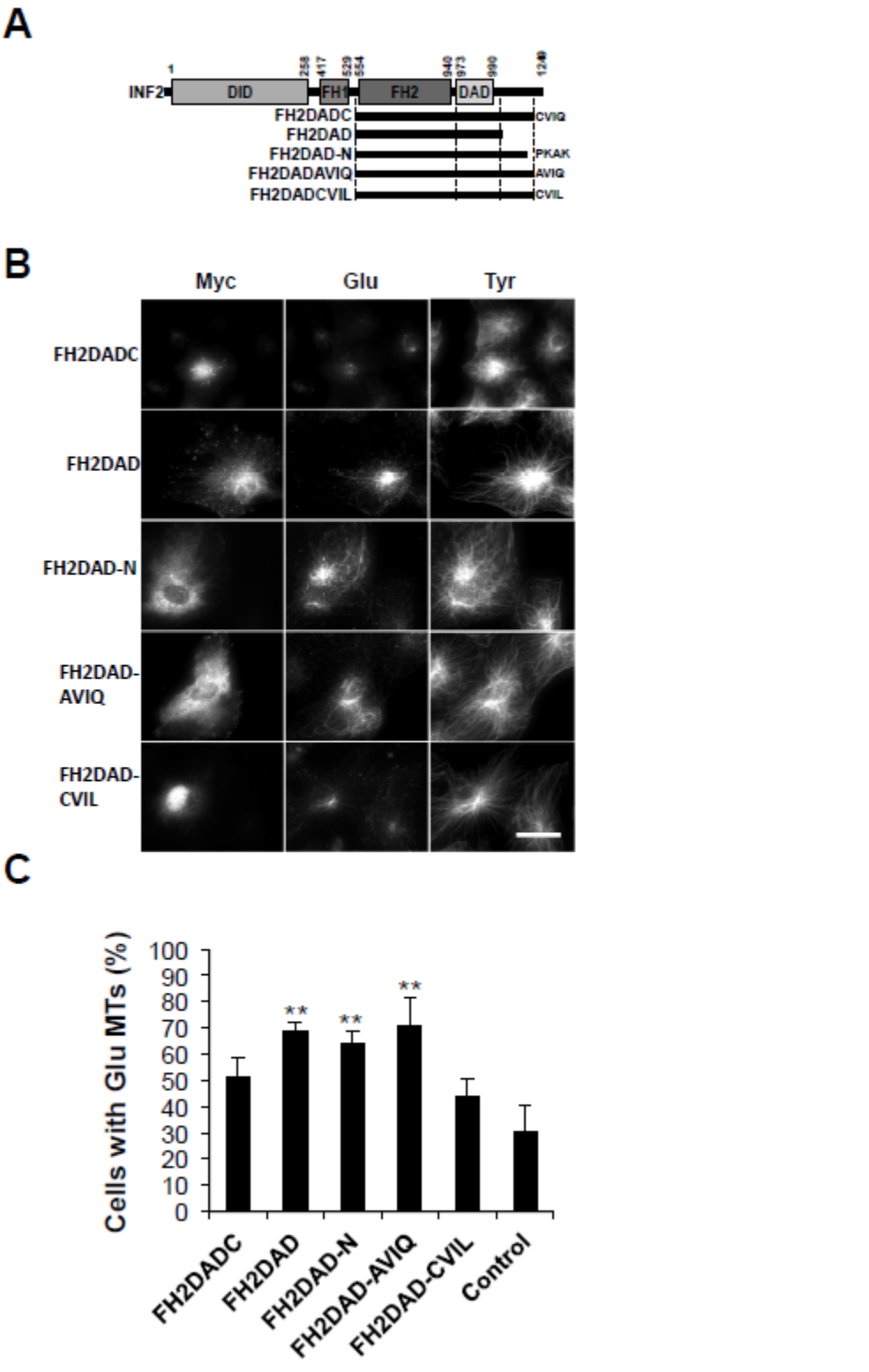

Figure S2. The presence of a CAAX box on active INF2 fragments inhibits Glu MT formation. (A) Schematic of the fragments of INF2 used in the experiment. FH2DAD-N

contains the C-terminus of an alternative splice variant of INF2 (INF2-2). In FH2DAD-AVIQ the C in the CAAX box was replaced by A to prevent farnesylation. In FH2DAD-CVIL the Q in the CAAX box was replaced by L to mimic the consensous sequence for geranylgeranylation. (B) Myc, Glu and Tyr tubulin staining of starved NIH3T3 fibroblasts expressing the indicated myc-tagged fragments of INF2. Bar, 20 μm (C) Quantification of cells with Glu MTs treated as in B; control refers to non-expressing cells. In all cases data are mean $\pm$ SEM from three independent experiments ($n > 50$ cells per experiment). **, $p < 0.001$, by chi-square test. Bar, 20 μm.

Figure S3

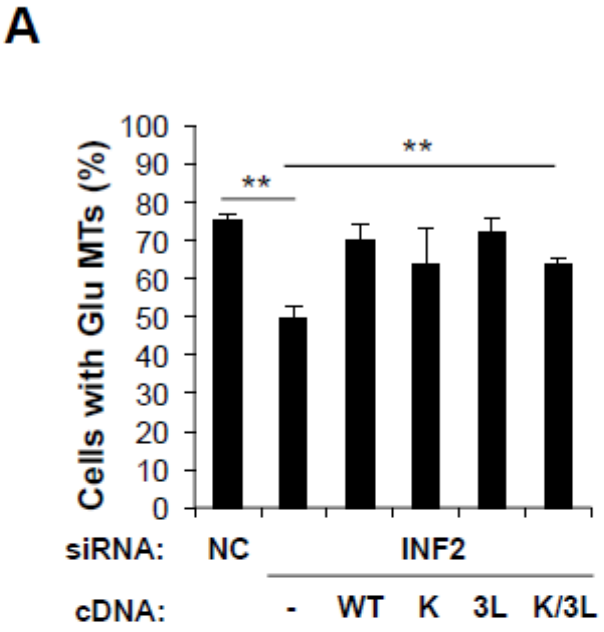

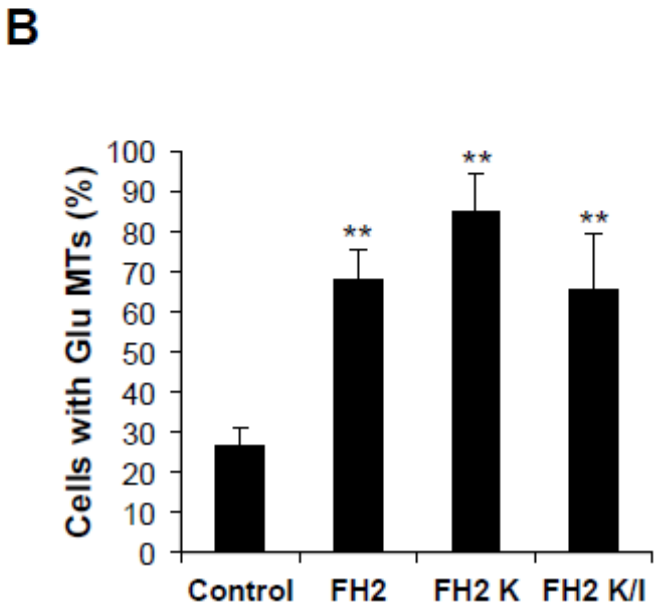

Figure S3. INF2 stabilizes MTs independently of its actin activities. (A) Quantification of serum grown NIH3T3 fibroblasts that exhibited Glu MTs after non coding (NC) or INF2 (INF2) siRNA treatment followed by expression of the indicated INF2 actin mutants (K, Lys^{792}; 3L, Leu^{976}, Leu^{977}, Leu^{986}; K3L, Lys^{792}, Leu^{976}, Leu^{977},

Leu[986]). (B) Quantification of starved NIH3T3 fibroblasts that exhibited Glu MTs after expressing the indicated FH2-INF2 actin mutant constructs (FH2K, Lys[792]; FH2K/I, Lys[792], Ile[643]). In all cases, data are mean ± SEM from three independent experiments (n> 50 cells per microinjection experiment in B and >200 cells/experiment in A). **, p< 0.001 by chi-square test.

Figure S4

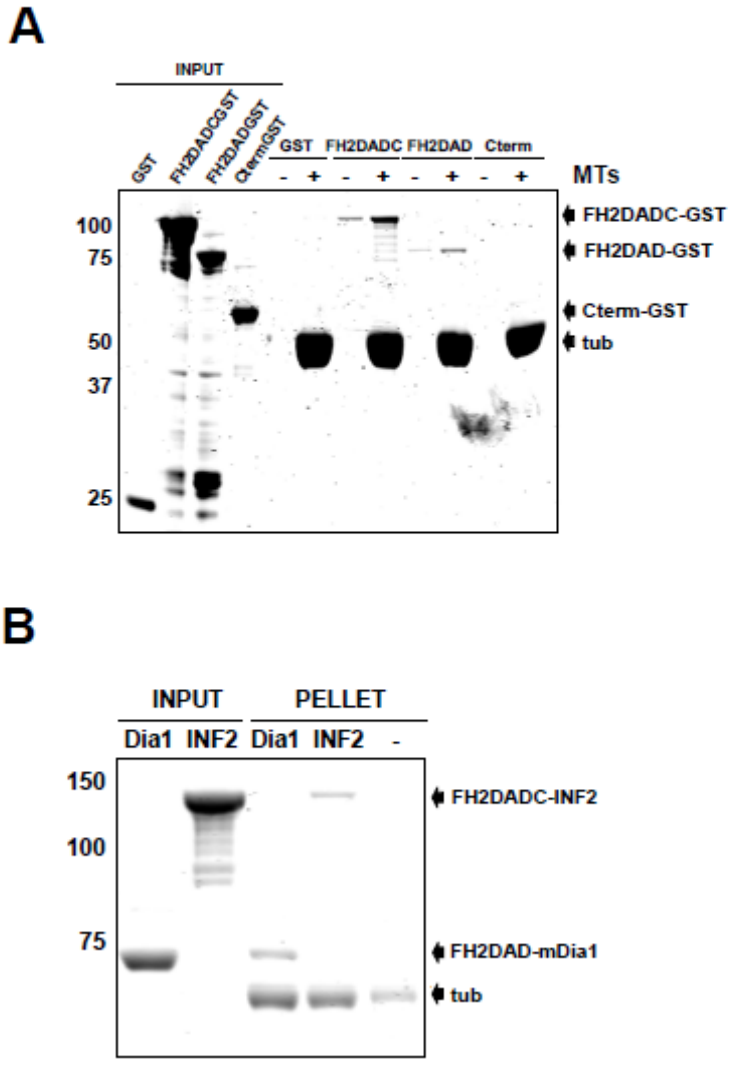

Figure S4. INF2 stabilizes MTs in vitro. (A) Coomassie staining of input proteins and pellets (on the right) after incubating the indicated GST-tagged INF2 proteins or GST with or without taxol stabilized MTs. (B) Coomassie staining input protein and MT pellets from reactions in which HIS-tagged mDia1FH2DAD (Dia1) or GST-tagged INF2FH2DADC (INF2) were incubated with spontaneously polymerizing tubulin before cold-induced depolymerization. tub, tubulin.

Figure S5

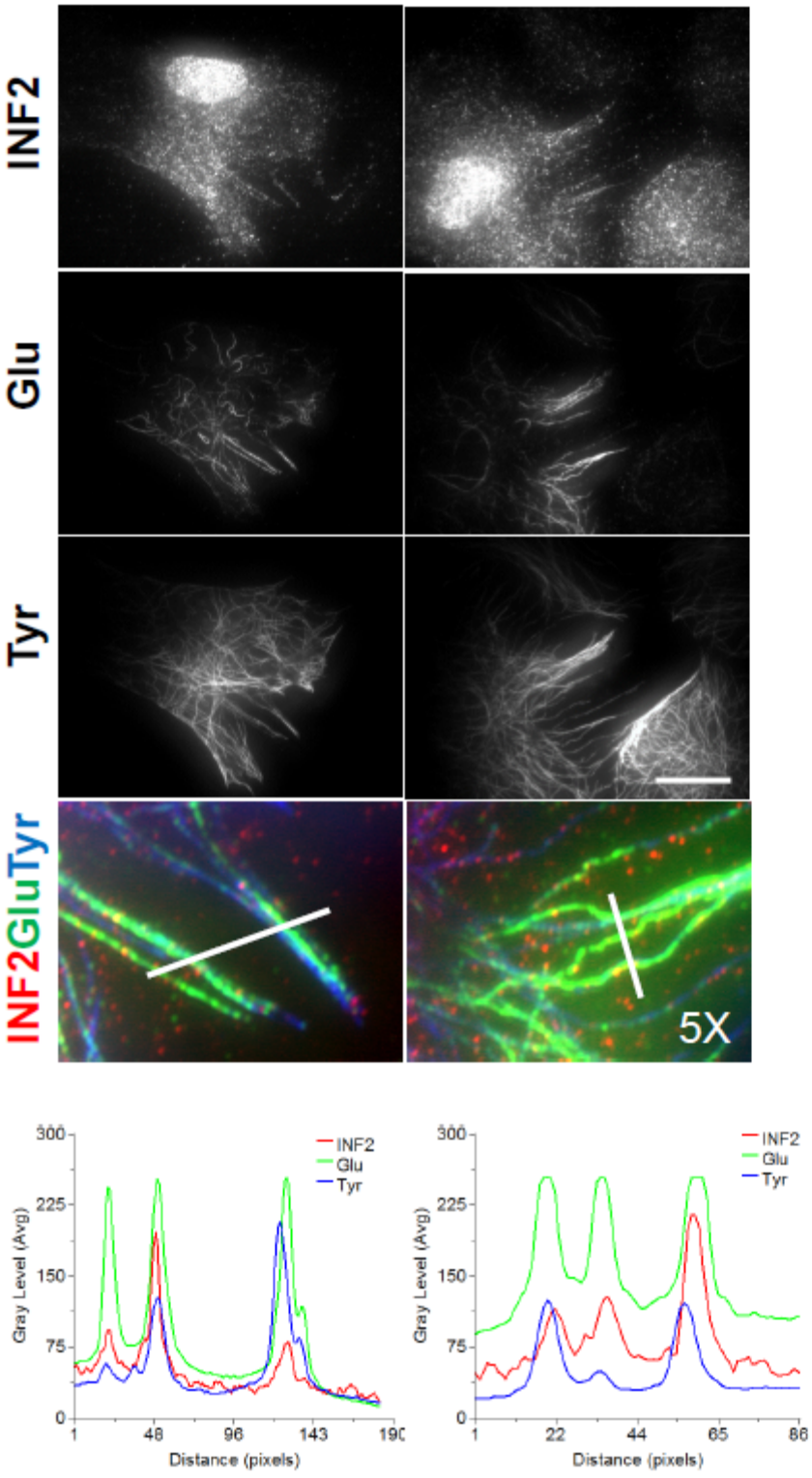
INF2
Glu
Tyr
INF2GluTyr
5X
INF2
Glu
Tyr
Gray Level (Avg)
Distance (pixels)
300
225
150
75
0
1
48
96
143
22
44
65

Figure S5. INF2 localizes to Glu MTs upon LPA stimulation. TIRF microscopy of LPA-stimulated NIH3T3 fibroblasts immunostained for INF2, Glu and Tyr tubulin. Separate fields are shown on the left and right panels. Bottom panels are quantification of INF2, Glu and Tyr tubulin fluorescence along the indicated white line on selected regions from TIRF images asindicated by a white line. Bar, 20 μm.

Figure S6

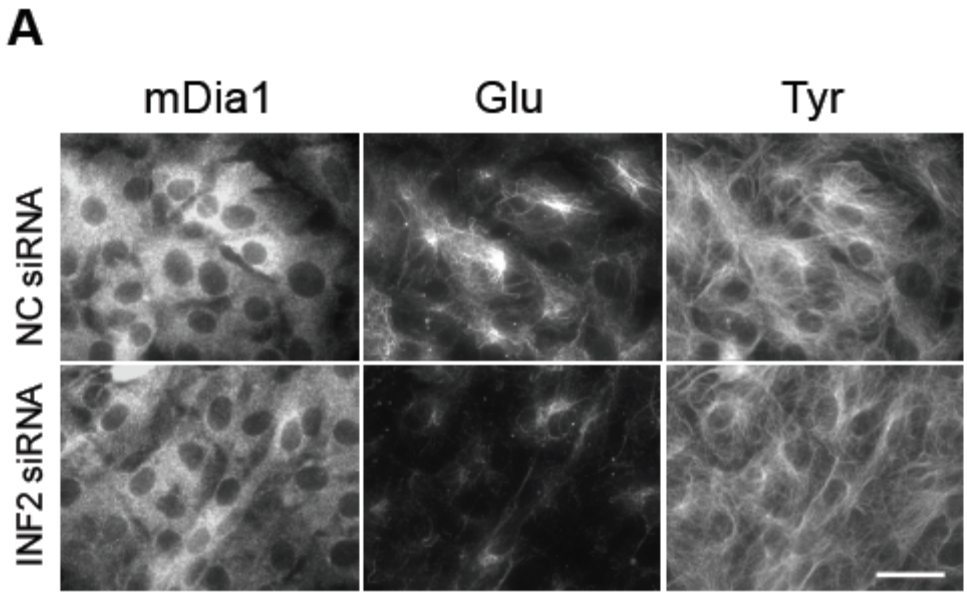

Figure S6. mDia1 localization is unaffected by INF2 knockdown. (A) Immunostaining of mDia1, Glu and Tyr tubulin in NIH3T3 fibroblasts treated with non-coding (NC) or INF2 siRNAs. Bar, 20 μm.

Figure S7

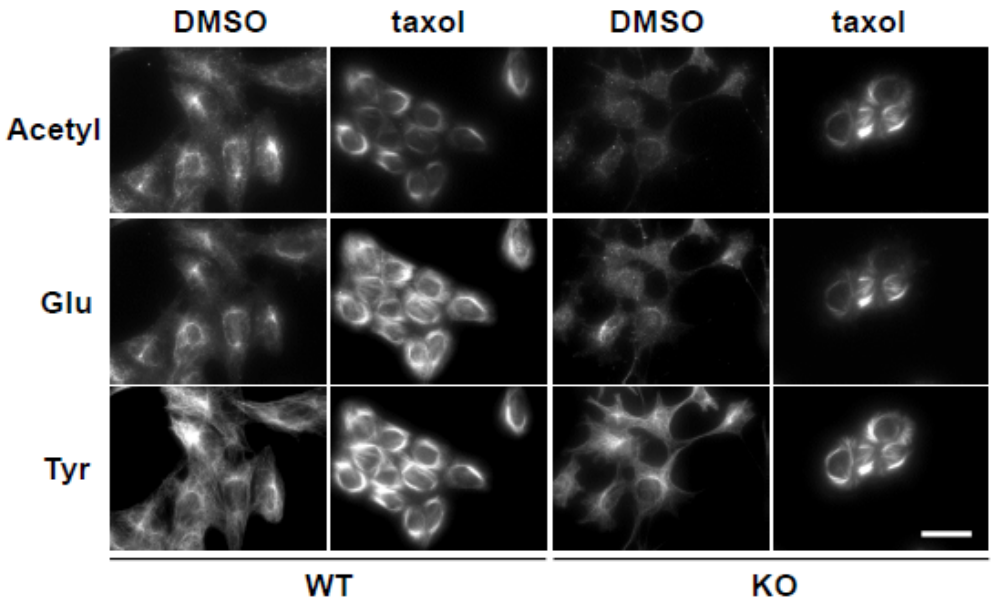

Figure S7. IQGAP1 KO MEFs are deprived of acetylated and Glu MTs but not tubulin modifying enzymes. Immunostaining of acetylated (Acetyl),Glu and Tyr tubulin in IQGAP1 WT and KO MEFs with or without incubation with 10 μM taxol for 1 hr. Bar, 20 μm.

Figure S8

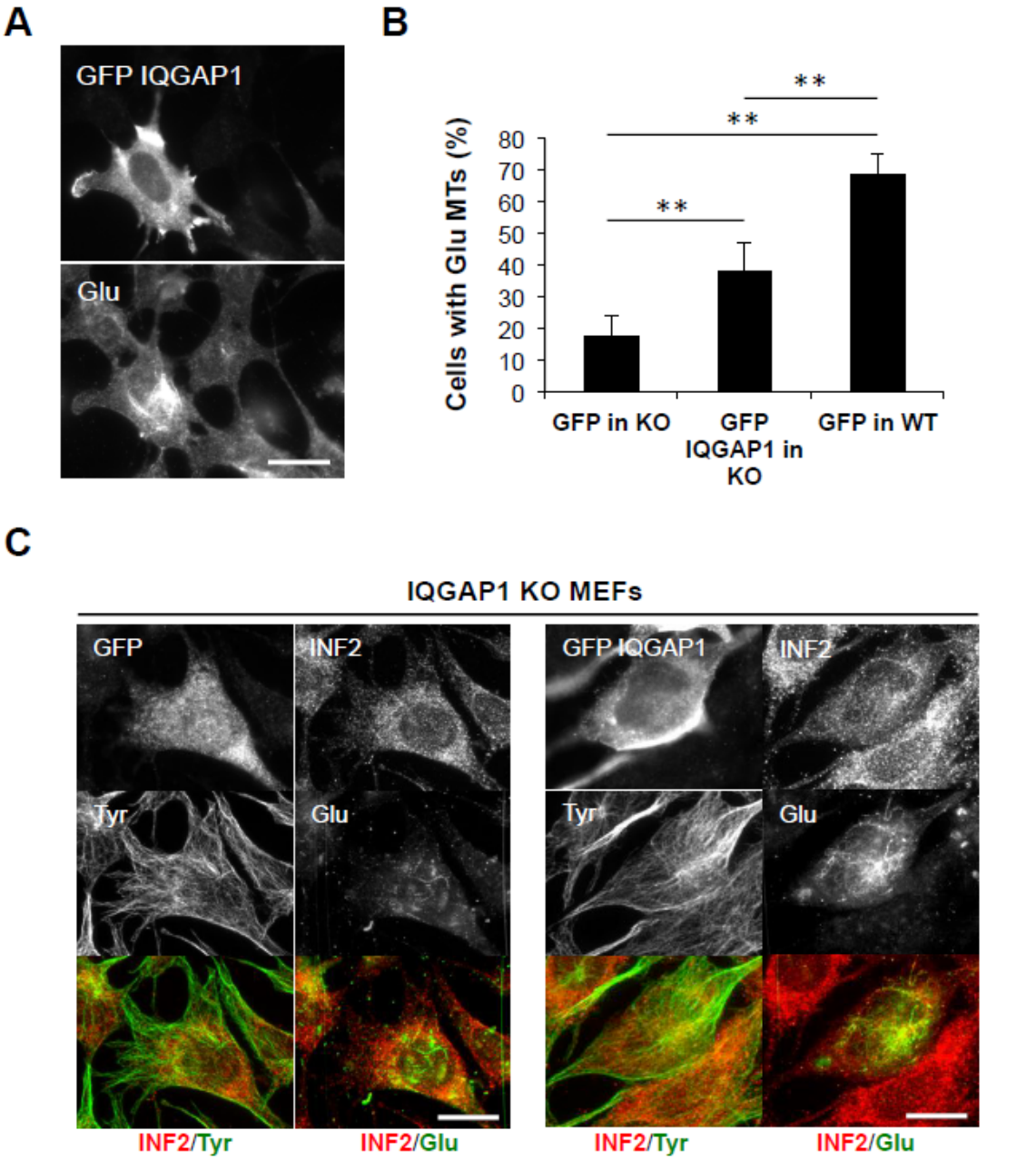

Figure S8. GFP-IQGAP1 expression rescues Glu MTs and INF2 localization in IQGAP1 KO MEF cells. (A) Immunostaining of GFP and Glu tubulin in IQGAP1 KO MEF cells expressing GFP-IQGAP1. (B) Quantification of cells with Glu MTs in cells treated as in A. In all cases data are mean ± SEM from three independent experiments (n> 50 cells per experiment). **, p< 0.001, by chi-square test.(C) Confocal microscopy of IQGAP1 KO cells transfected with either GFP or GFP-IQGAP1 and immunostained with INF2, GFP, Glu and Tyr tubulin antibodies. Maximum projection images are shown. Bars, 20 µm.

Figure S9

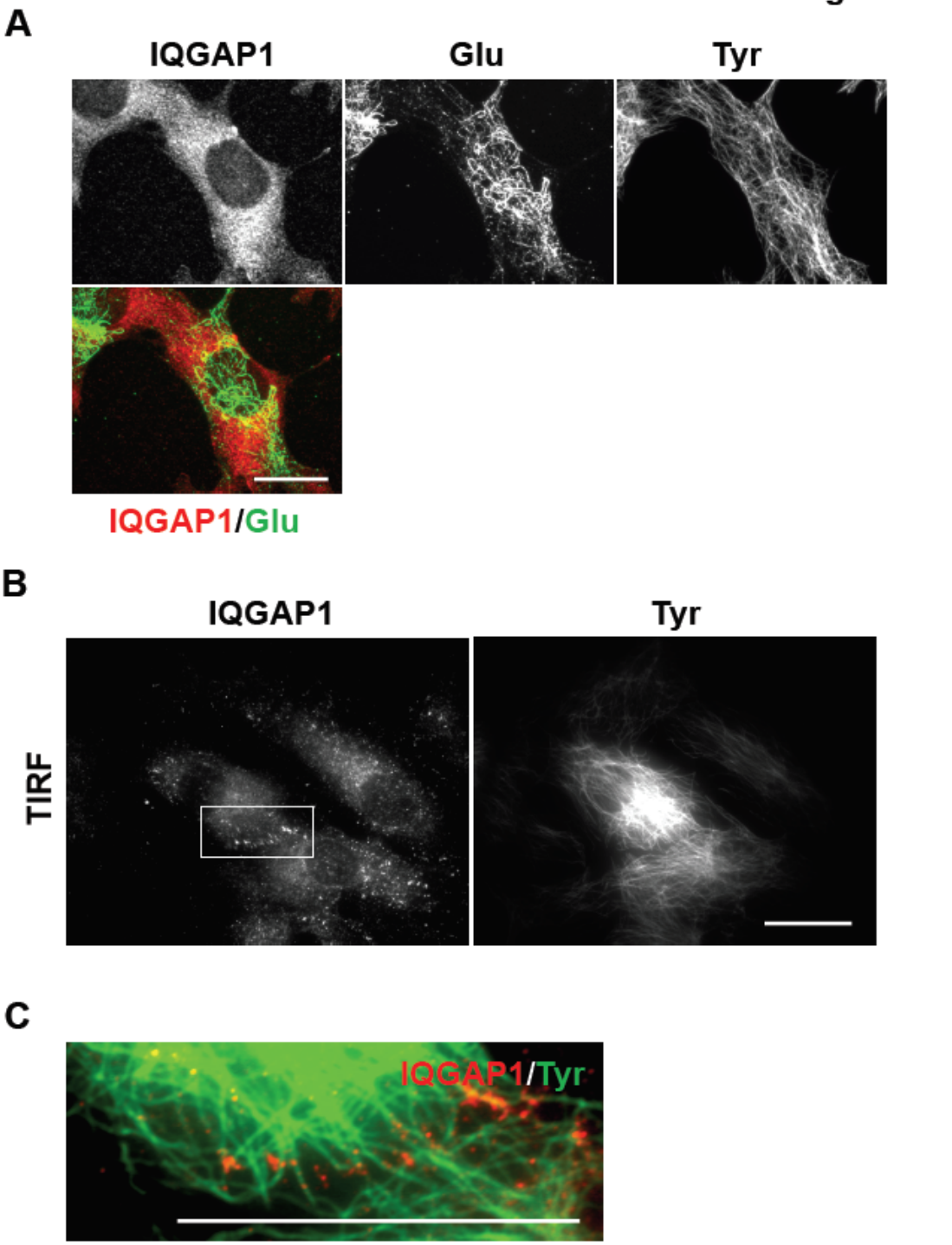

Figure S9. IQGAP1 co-localizes with cortical dynamic MTs. (A) Confocal microscopy of endogenous IQGAP1, Glu and Tyr tubulin in NIH3T3 fibroblasts. Maximum projection images are shown.(B) TIRF microscopy of endogenousIQGAP1 and Tyr tubulin in NIH3T3 fibroblasts. (C) Magnification of the region boxed as in A showing merged IQGAP1 and Tyr MT signals. Bars, 20 µm.

Table 1. Parameters of MT dynamic instability in cells depleted of INF2 or mDia1

	NC	siINF2	simDia1
growth rate (µm/min)	4.36 ± 0.26	7.74 ± 0.35 ****	7.63± 0.26 ****
shrinkage rate (µm/min)	4.81 ± 0.27	8.01 ± 0.46 ***	7.43 ± 0.31 ****
catastrophe frequency (min^{-1})	3.54 ± 0.19	3.91 ± 0.17	3.94 ± 0.12
rescue frequency (min^{-1})	3.65 ± 0.36	3.30 ± 0.24	4.05 ± 0.21
% growth	33.12 ± 2.15	41.33 ± 1.54**	37.82 ± 2.04
% shrinkage	31.73 ± 2.03	39.82 ± 1.64**	40.63 ± 1.84**
% time pausing	35.21 ± 2.37	19.62 ± 2.33 ****	21.68 ± 1.82 ***
MT lifetime (min)	2.00 ± 0.-09	1.85 ± 0.06	1.83 ± 0.04
MT dynamicity (µm/min)	3.01 ± 0.21	6.41 ± 0.35 ****	5.93 ± 0.26 ****
number of MTs	20	20	20

MT dynamics (mean ± SEM) in RFP-tubulin NIH3T3 cells transfected for 72 h with non-coding control siRNA (NC) or either siRNA to silence Dia1 (simDia1) or INF2 (siINF2). ****, $p<0.0001$, ***, $p<0.001$, **, $p<0.01$, *, $p<0.05$ by two-tailed student's t-tests. No asterisk means $p>0.05$. Dynamicity is calculated by dividing the sum of growth and shrinkage distances by MT lifetime.

Table S2. Parameters of MT dynamic instability in cells depleted of INF2 or mDia1 and expressing DAD domains

	NC siRNA		
	GFP	**INF2 DAD**	**mDia1 DAD**
growth rate (μm/min)	4.69 ± 0.26	4.93 ± 0.21	4.35 ± 0.19
shrinkage rate (μm/min)	5.04 ± 0.22	4.88 ± 0.17	4.67 ± 0.19
catastrophe freq. (min^{-1})	3.60 ± 0.19	3.70 ± 0.16	3.61 ± 0.18
rescue freq. (min^{-1})	3.62 ± 0.36	3.85 ± 0.14	3.55 ± 0.16
% growth	34.67 ± 1.92	32.34 ± 2.12	29.40 ± 1.35
% shrinkage	31.74 ± 2.04	32.60 ± 1.65	32.81 ± 1.73
% time pausing	33.26 ± 2.20	35.22 ± 2.59	37.79 ± 1.96
MT lifetime (min)	2.05 ± 0.08	1.95 ± 0.07	1.93 ± 0.07
MT dynamicity (μm/min)	3.25 ± 0.20	3.18 ± 0.16	2.78 ± 0.10 *
number of MTs	20	20	20
	INF2 siRNA		
	GFP	**INF2 DAD**	**mDia1 DAD**
growth rate (μm/min)	7.91 ± 0.35 ****	8.07 ± 0.36 ****	8.56 ± 0.42 ****
shrinkage rate (μm/min)	7.84 ± 0.37 ****	8.25 ± 0.56 ****	8.17 ± 0.35 ****
catastrophe freq. (min^{-1})	3.88 ± 0.13	3.65 ± 0.15	3.64 ± 0.17
rescue freq. (min^{-1})	3.50 ± 0.25	3.55 ± 0.19	3.53 ± 0.15
% growth	40.44 ± 1.75*	38.75 ± 1.46	41.87 ± 1.63**
% shrinkage	39.32 ± 1.68**	41.51 ± 1.58***	40.26 ± 2.5*
% time pausing	20.92 ± 2.31 ***	19.74 ± 1.85 ***	19.86 ± 1.81 ***
MT lifetime (min)	1.91 ± 0.07	1.95 ± 0.05	1.92 ± 0.07
MT dynamicity (μm/min)	6.33 ± 0.34 ****	6.55 ± 0.35 ****	6.87 ± 0.38 ****
number of MTs	20	20	20
	mDia1 siRNA		
	GFP	**INF2 DAD**	**mDia1 DAD**
growth rate (μm/min)	7.77 ± 0.29 ****	5.18 ± 0.27	8.30 ± 0.32 ****
shrinkage rate (μm/min)	7.56 ± 0.29 ****	4.99 ± 0.25	8.54 ± 0.44 ****
catastrophe freq. (min^{-1})	3.87 ± 0.12	3.61 ± 0.14	3.67 ± 0.19
rescue freq. (min^{-1})	3.99 ± 0.24	3.43 ± 0.19	3.72 ± 0.19
% growth	39.00 ± 1.74	36.20 ± 1.26	37.42 ± 1.58
% shrinkage	40.34 ± 1.69**	37.14 ± 1.96	43.60 ± 2.22***
% time pausing	20.78 ± 1.92 ***	26.47 ± 1.70	19.20 ± 1.58 ****
MT lifetime (min)	1.87 ± 0.04	1.93 ± 0.06	1.91 ± 0.05
MT dynamicity (μm/min)	6.12 ± 0.27 ****	3.79 ± 0.22 ****	6.87 ± 0.38 ****
number of MTs	20	20	20

MT dynamics (mean ± SEM) in RFP-tubulin NIH3T3 cells transfected with non-coding control siRNA (NC) or either siRNA to silence Dia1 (simDia1) or INF2 (siINF2) and expressing mDia1-DAD or INF2-DAD. Statistics were performed by 2-way ANOVA with Tukey's multiple comparison test comparing different groups to GFP NC siRNA. * $p<0.05$, *** $p<0.001$; **** $p<0.0001$. No asterisk means $p>0.05$. Dynamicity is calculated by dividing the sum of growth and shrinkage distances by MT lifetime.

Supplemental Material and Methods

MT binding and stability assays

DEAE-purified tubulin (prepared as described in Mikhailov et al., 1995) was polymerized at a concentration of 25 µM inPEMG buffer (100 mM Pipes-KOH, pH 6.9, 1 mM EGTA, 2 mM $MgCl_2$, and 1 mM GTP) in the presence of 10 µM Taxol at 37 °C for 1 h. MTs (12.5 µM) were incubated with 1 µM of purified GST-INF2 fragments or GST alone for 10 min at 30 °C. MTs were isolated by centrifugation at 100,000 *g* for 10 min at 37 °C, and matching aliquots of supernatant and pellets loaded onto SDS-PAGE for protein detection by Coomassie staining. To assess MT stability to cold-induced depolymerization, DEAE tubulin at 25 µM was induced to polymerize in PEMG buffer with 10% DMSO in the presence of 2 µM HIS-mDia1, GST-INF2 or BSA alone for 1 h at 37 °C before 30 min incubation at 4 °C. Cold-stable MT pellets were isolated by centrifugation (100,000*g* for 10 min) and matching aliquots of input reactions and pellets resolved on 10% SDS-PAGE to detect proteins by Coomassie staining.

Confocal microscopy

Fixed and immunostained samples were observed using an Olympus IX83 microscope with wide field and DSU spinning disk imaging. The microscope was equipped with IX3-RFA Straight illuminator, 60 X Plan Apo oil objective (NA 1.3) and ORCA R2 Deep cooled CCD camera (Hamamatsu) and controlled by Metamorph imaging software. Z-stack images were taken at 0.2µm steps for 15-20 stacks and a maximum projection was generated.

Supplemental Reference

Mikhailov, A.V., and Gundersen, G.G. (1995). Centripetal transport of microtubules in motile cells. Cell motility and the cytoskeleton *32*, 173-186.